ARTICLE NO. 79-4121

Two-Dimensional Mathematical Model of a Nonbuoyant Jet in a Crossflow

Milorad Lj. Bojić*
Masinski Fakultet, Univerzitet Svetozar Markovič Kragujevac, Yugoslavia
and
S. Eskinazi†
Syracuse University, Syracuse, N.Y.

The mean velocity distribution for the mixing of a turbulent, nonbuoyant, round jet in a cross wind is calculated using a two-dimensional mathematical model (on the plane of symmetry) based on a linear superposition of the developments of the jet, the two bound vortices formed from the rolling up of the vorticity in the initial stage of the jet, the wake behind the bent jet, and the freestream. The results of the mathematical model are compared with measurements of the mean velocity on the same plane of symmetry. These comparisons, which are performed for a jet to freestream velocity ratio of 3.87 and a jet Reynolds number 4.74×10^4, show a relatively good first-order agreement between the model and the experimental results. The analysis includes prior models of centerline geometry and mean speeds, and extends the predictions of mean speeds to the entire plane of symmetry where the jet centerline is located.

Nomenclature

d = diameter of pipe
DZ' = dimensionless distance to jet centerline
r' = dimensionless radial distance, r/d
$r'_{1/2}$ = dimensionless radial distance where $U_j = U_{jm}/2$
R = radial distance from axis of vortex (Fig. 3)
R' = dimensionless radial distance from axis of vortex (Fig. 3)
t = time
T = rms of turbulent velocity
U = velocity
U_∞ = freestream velocity
U_{jav} = spatial average velocity of jet
U_j = jet velocity on plane of symmetry
U_{jm} = maximum jet velocity on plane of symmetry
U_v = induced velocity by bound vortices
U_w = wake velocity
U_1 = combined velocity of jet and bound vortices
X' = dimensionless coordinate in freestream direction
Y' = dimensionless coordinate normal to freestream and axis of pipe
Z' = dimensionless coordinate along axis of pipe
γ = angle in Fig. 2
Γ = circulation
Γ_0 = circulation at jet axis
ζ' = dimensionless distance along jet centerline (Fig. 2)
ϵ = angle of spread of jet
Λ = Lagrangian macroscale
ν_τ = turbulent eddy viscosity
ξ' = dimensionless distance to jet centerline (Fig. 2)

Subscripts

e = arbitrary point E in the field of Fig. 2
h = bound vortex centerline

Received Aug. 4, 1978; revision received April 26, 1979.

Index categories: Nozzle and Channel Flow; Atmospheric and Space Sciences; Thermal Modeling and Analysis.

*Teaching Assistant.
†Professor, Dept. of Mechanical and Aerospace Engineering.

I. Introduction

THERE is a considerable amount of work published on the flow resulting from the mixing of a round jet issuing into a uniform crossflow. There does not seem to be quantitative agreement in the generalization of the experimental data and mathematical models that have been proposed. The most important concept that has been omitted in previous modeling of the mixing of these flows is its strong three-dimensional character, and especially the influence of the pair of bound vortices on the lee side of the jet.

Most of the existing mathematical models for this type of flow, such as those by Morton,[1] Hoult et al.,[2] and a number of other investigators, are given for a one-dimensional "top hat" velocity, momentum, and energy distribution across the jet. Basically, they can be considered as one-dimensional in the direction of the intrinsic coordinate of the jet centerline.

The presence of the bound-vortex system on the lee side of the jet was observed by Pratte and Baines,[3] studied by Durando,[4] and later quantified by Moussa et al.[5] Little or nothing was done to incorporate the influence of the bound vortex system in dealing with the mathematical modeling of this mixing process.

To the authors' best knowledge, this is the first time that a two-dimensional mathematical model in the plane of symmetry has been proposed that takes into account the effect of the jet diffusion and the influence and development of the bound vortex system, the wake, and the freestream.[6]

II. Mathematical Model

Figure 1 is a schematic representation of the nonbuoyant turbulent jet with a spatial average velocity U_{jav} issuing from a round pipe of outside diameter d mixing with a uniform, parallel crossflow with velocity U_∞. The length of this pipe was chosen such that the flow just before the exit is a fully-developed turbulent flow, thus avoiding the influence of the development of a potential core. This figure also shows the Cartesian coordinate system made dimensionless with the diameter of the pipe, and the lines $X' = 1$, 2, and 3 on the plane of symmetry ($Y' = 0$), along which the measured and computed mean velocity distributions have been obtained. The mathematical model to be developed is based on a linear superposition of the developments of the jet, the two bound vortices formed by the rolling up of the vorticity in the initial stage of the jet, the wake behind the bent jet, and the freestream.

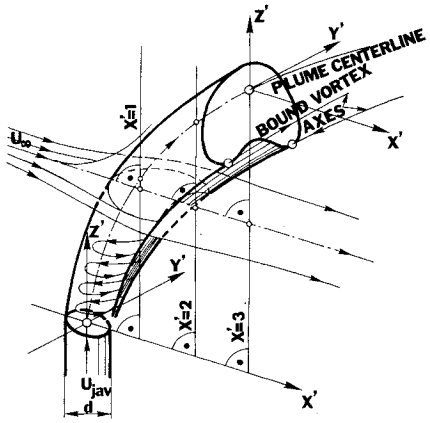

Fig. 1 Flow descriptions and coordinates.

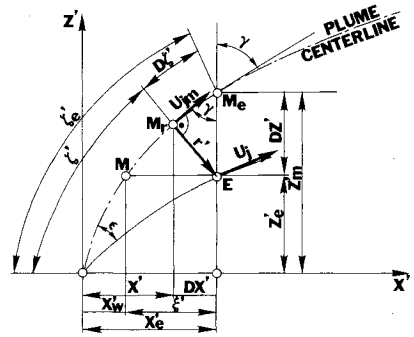

Fig. 2 The plane $Y'=0$.

A. Jet Region

The geometry on the plane $Y'=0$ is shown in Fig. 2. The plume centerline, defined as the locus of the maximum velocity on that plane, is shown together with an arbitrary point $E(X_e', 0, Z_e')$ where the mean velocity is to be computed.

Since the investigations of Chassaing et al.[7] were conducted under conditions very similar to those in this study, their plume centerline geometry, maximum velocity, and width development expressions will be used:

$$Z' = (0.999 + 0.588\, U_{jav}')\,(X')^{0.385} \tag{1}$$

$$U_{jm} = U_{jav} 0.70 (X')^{-0.51} \tag{2}$$

$$r_{1/2}' = 0.37 (X')^{0.75} \tag{3}$$

Here, $U_{jav}' = U_{jav}/U_\infty$ is the dimensionless spatial mean velocity of the jet, $r_{1/2}'$ is the dimensionless radius r/d at which $U_j = U_{jm}/2$. Equations (2) and (3) are developed from Chassaing for $U_{jav}' = 3.95$, $d = 4$ cm, and $X' > 0.5$. Nevertheless, these general similarity relations have been investigated by them for a range of conditions: $21{,}200 < Re < 53{,}600$, $2.37 < U_{jav}' < 6.35$, and $0.5 < X' < 6$. Furthermore, the form of Eq. (1) has been found by a number of investigators to be valid for higher values of U_{jav}'. The dimensionless development of Chassaing's jet region is considered to be identical to that of this study because of the closeness of the Reynolds number from which Eqs. (2) and (3) were developed.

As in the case of an axisymmetric jet, we assume that the contribution of the jet part of the flow is in any plane normal to the jet centerline, given by the Reichardt[8] distribution:

$$U_j = U_{jm} \exp[-0.69 (r'/r_{1/2}')^2] \tag{4}$$

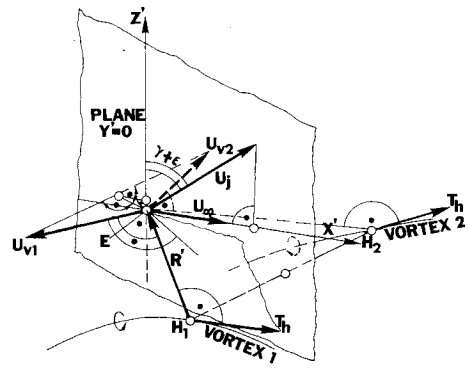

Fig. 3 Vectorial velocity superposition for the point E.

or using the geometry of Fig. 2

$$U_j = 0.7 U_{jav} (X_e' - DZ' \sin\gamma \cos\gamma)^{-0.51} \times \exp[-5.04 (DZ' \sin\gamma)^2 / (X_e' - DZ' \sin\gamma\cos\gamma)^{1.5}] \tag{5}$$

where

$$\gamma = \tan^{-1} [dZ'(X_e')/dX']^{-1}$$

The jet angle of spread ϵ is approximated as:

$$\epsilon = \tan^{-1} (r'/\zeta') \tag{6}$$

From Fig. 2, this angle becomes

$$\epsilon = \tan^{-1} [DZ' \sin\gamma / (\zeta_e' - DZ' \cos\gamma)] \tag{7}$$

where

$$\zeta_e' = \int_0^{X_e'} [1 + (dZ'(X_e')/dX')^2]^{1/2} dX'$$

B. Bound Vortex Region

The bound vortex system is a pair of semi-infinite curved-line vortices equidistant from the plane of symmetry and with opposite rotation. This system was found by Moussa et al.[5] to originate at the discharge of the jet from the vorticity in the boundary layer on the inside wall of the pipe.

It is assumed that the circulation Γ in this continuous vortex tube decays with time t and position R, according to the axisymmetric solution for an infinitely long rectilinear vortex[9]

$$\Gamma = \Gamma_0 [1 - \exp(-R^2/4\nu_\tau t)] \tag{8}$$

Here, Γ_0 is the initial circulation and ν_τ is the turbulent eddy kinematic viscosity. This initial circulation is taken as the integrated vorticity in the inside boundary layer at the half-exit of the pipe. This value was given by Moussa et al.[5] to be 1.12 m^2/s for $U_{jav}' = 3.48$ and the same pipe diameter. The value of U_{jav}' in this study was stated to be 3.87, and is considered to be sufficiently close to 3.48 to assume the same Γ_0.

The dimensionless radial distance $R' = V_e - V_h$ is found from the geometrical relationships shown in Fig. 3. Here, V_e and V_h are position vectors of points E and $H_1(X_h', Y_h', Z_h')$, respectively.

Through measurements discussed in Sec. IVA for injection normal to U_∞, the vortex centerline was found to be described by this set of parametric equations:

$$Y_h' = 0.145\, X_h'^2 - 0.865\, X_h' - 0.122 \tag{9}$$

$$Z_h' = -0.0922\, X_h'^2 + 1.18\, X_h' + 0.467 \tag{10}$$

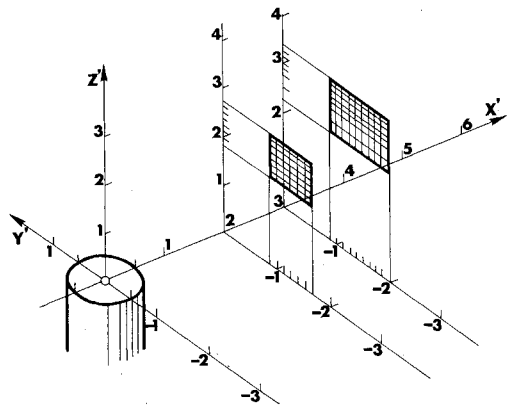

Fig. 4 Two two-dimensional matrices of measurement points with the pressure probe for $X'=2$ and $X'=3$.

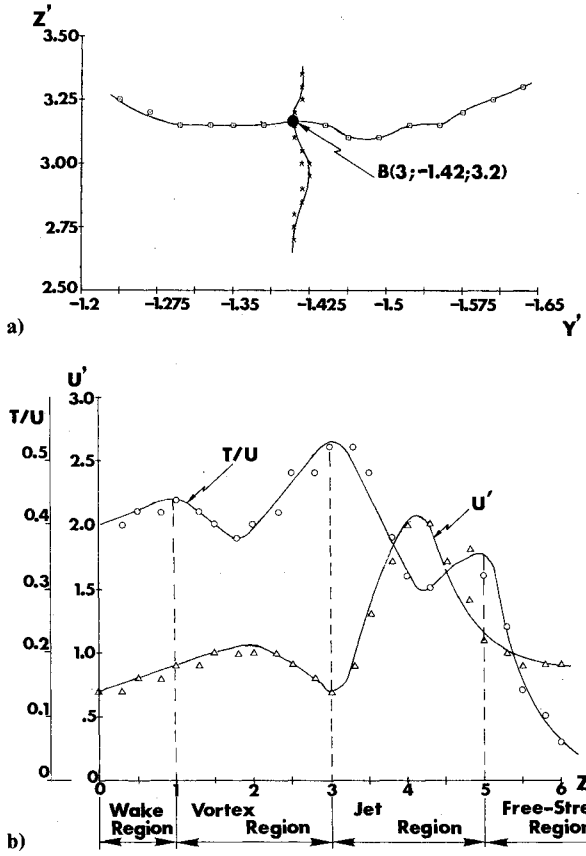

Fig. 5 a) Vortex centerline point in the plane $X'=3$. b) U' and T/U vs Z' for $Y'=0$ and $X'=2$.

These equations are valid for $X'_h \geq 0.5$. Using Eqs. (9) and (10) and the condition for $\boldsymbol{R}'$ to be perpendicular to the vortex centerline $\boldsymbol{R}' \cdot \boldsymbol{T}'_h = 0$ gives

$$X'^3_h - 11.9\,X'^2_h + (51.2 + 3.12\,Z'_e)\,X'_h + (11.1 - 16.9\,X'_e - 20\,Z'_e) = 0 \tag{11}$$

Using a calculated value of X'_h from Eq. (11), the value R' can be obtained.

The turbulent eddy viscosity ν_T appearing in Eq. (8) is taken to be constant and is determined by best fit of model to the experiments. This best-fit value was found to be in some order-of-magnitude agreement with the turbulent eddy viscosity calculated by Eskinazi and Moussa from the turbulence structure, and as yet unpublished. This can easily be verified if ν_T is defined on the basis of Lagrangian correlation for large times as $T\Lambda$, where T is the average turbulent velocity and Λ is the average integral scale of the turbulence which must be of the order of the pipe diameter 0.0254 m. The average value of T can be selected from Fig. 5b to be about $0.45 \times 2.95 \simeq 1.33$ m/s.

The time of the diffusion t has been replaced in this model by

$$t = X_h / U_\infty \tag{12}$$

Thus, it is assumed in this time evaluation that $U_X \simeq U_\infty$.

The magnitude of the induced velocities $|U_{v1}|$ and $|U_{v2}|$ can be obtained from the solution of rectilinear viscous vortex[9]:

$$U_v = (\Gamma/2\pi R)\,[1 - \exp(\mathrm{d}R'^2 U_\infty / 4\nu_T X'_h)] \tag{13}$$

C. Wake Region

Since the jet is taken as an obstacle to the freestream, a wake is formed behind the jet. Therefore, the wake influence on the total velocity distribution is taken into account. The wake velocity deficiency at the center of the wake is[10] (see Fig. 2):

$$U'_w = C'/(2X'_e - \xi')^{1/2} \quad \text{for} \quad \xi' < 2X'_e \tag{14}$$

Here, C' is assumed to be the same parametric constant for every field point E with the same X'_e, and thus computed from an experimental data point at $E_0\,(X'_e, 0, 0)$ as[6]:

$$C' = [(U')_0 - (U'_l)_0]\,(X'_e)^{1/2} \tag{15}$$

Here, $(U')_0$ is the magnitude of the total velocity vector at E_0. U'_l is the value of the velocity at the same point computed from the mathematical model.

D. Velocity Superposition

In the freestream region, the velocity is constant. On the plane of symmetry and planes $X' = \text{const}$, the mathematical model for the dimensionless velocity distribution $U' = U/U_\infty$ vs Z' is assumed to be the vectorial superposition of the velocity contributions in the regions defined previously.

In the wake and vortex region, the jet velocity distribution U_j and the induced velocities of the pair of bound vortices 1 and 2, U_{v1} and U_{v2} are added vectorially as (Fig. 3):

$$\boldsymbol{U}'_l = \boldsymbol{U}'_j + \boldsymbol{U}'_{v1} + \boldsymbol{U}'_{v2} \tag{16}$$

In X', Y', and Z' component form

$$U_{lX'} = U_j \sin(\gamma + \epsilon) + 2U_{vX'}, \quad U_{lY'} = 0$$

and

$$U_{lZ'} = U_j \cos(\gamma + \epsilon) + 2U_{vZ'} \tag{17}$$

Then the magnitude of U'_l is added to the wake velocity

$$U' = U'_w + |U'_l| \tag{18}$$

Although U'_w is not necessarily in the direction of U'_l, an algebraic addition is employed in Eq. (18) because the direction of U'_w is not readily known without experiments.

Since the wake influence does not extend to the jet and freestream regions on the $Y' = 0$ plane, the velocity of the flow there can exclude the wake influence

$$U_j = [0.7\,U_{jav}\,(X'_e - DZ' \sin\gamma \cos\gamma)^{-0.51} - U_\infty \sin(\gamma + \epsilon)] \times \exp[-5.04\,(DZ' \sin\gamma)^2 / (X'_e - DZ' \sin\gamma \cos\gamma)^{1.5}] \tag{19}$$

$$U = U_j' + U_{v1}' + U_{v2}' + U_\infty' \tag{20}$$

where

$$U_{X'} = U_j \sin(\gamma + \epsilon) + 2U_{vX'} + U_\infty$$
$$U_{Y'} = 0, \qquad U_{Z'} = (U_l)_{Z'} \tag{21}$$

III. Experimental Equipment

A 2.54-cm o.d., 2.36-cm i.d., and 60.96-cm stainless steel pipe supplied the jet flow. The pipe centerline was halfway between the walls of the wind tunnel. The average jet speed at the pipe exit was maintained at 2.95 m/s for all measurements. To simulate a natural environment, the tunnel walls diverged slightly to maintain a constant static pressure.

A. Pressure Probe Measurements

The pressure probe used is a three-dimensional probe with a 0.32-cm-diam (United Sensor and Control Corp.). It is designed for flow angle measurements. During the measurements, the probe was moved in the X' and Y' directions without rotation so that the hole always faced the $-X'$ direction. Measurements in Z' were obtained by moving with a screw mechanism the pipe discharge in the Z' direction. The pressures were measured by an inclined multitube manometer.

Figure 4 shows a two-dimensional matrix of the measurement points in planes $X' = \text{const}$. For the plane $X' = 2$ there were 56 measurement points, and for $X' = 3$, there were 80 measurement points.

B. Hot-Wire Measurements

For velocity measurements, a 5-μm-diam, 1.25-mm-long hot wire (Disa model 55A22) was used as a sensor. To minimize the probe stem interference with the sensing hot wire, a right-angle adapter (Disa model 55A27) was used. The mean values of the linearized and nonlinearized signals were read through two digital voltmeters and, simultaneously, the rms value of the linearized signal was read through a true rms voltmeter.

IV. Experimental Results and Analysis

A. Points on the Vortex Centerline

The pressure data obtained were mathematically processed to determine vortex centerline points on the basis of maximum pressure difference criteria. The mathematical procedure used for obtaining a functional expression for the vortex centerline in planes $X' = \text{const}$ is as follows:

1) Differences d_{ij} of the pressures p_{ij} measured by the probe inside the matrices of Fig. 4 with the pressure at the boundary points of the matrix were calculated.

2) Differences found in step 1 as a function of Y' for $Z' = \text{const}$, and as a function of Z' for $Y' = \text{const}$ are fitted with a second-degree polynomial. Subsequently, Y' values for the extremum of these polynomials for different Z''s are found, and this forms the first Z' vs Y' set of extrema in the X' plane. The same was done for the set of Z' values of extrema of these polynomials for different $Y' = \text{const}$.

3) Cubic spline fits for the two sets of extrema, Z' vs Y' and Y' vs Z', are plotted. The point of the intersection being the maximum of the extrema is taken as the point on the vortex centerline (see Fig. 5a).

The procedure just explained was developed for experimental data measured in planes $X' = 2$ and $X' = 3$, and the coordinates of the vortex centerline (2, -1.25, 2.42) and (3, -1.42, 3.20) were obtained. These coordinates of vortex centerline were used, together with Moussa's values of (0.5, -0.5, 1) and (1, -0.875, 1.625) in planes $X' = 0.5$ and 1, to obtain the parametric centerline, Eqs. (9) and (10). To a large extent, the analysis presented here applies to the near field of the flow defined in this paper as $X' \leq 3$. When one is interested in the far field, the model basically transforms itself to a pair of line vortices in a freestream close to a Beltrami flow.

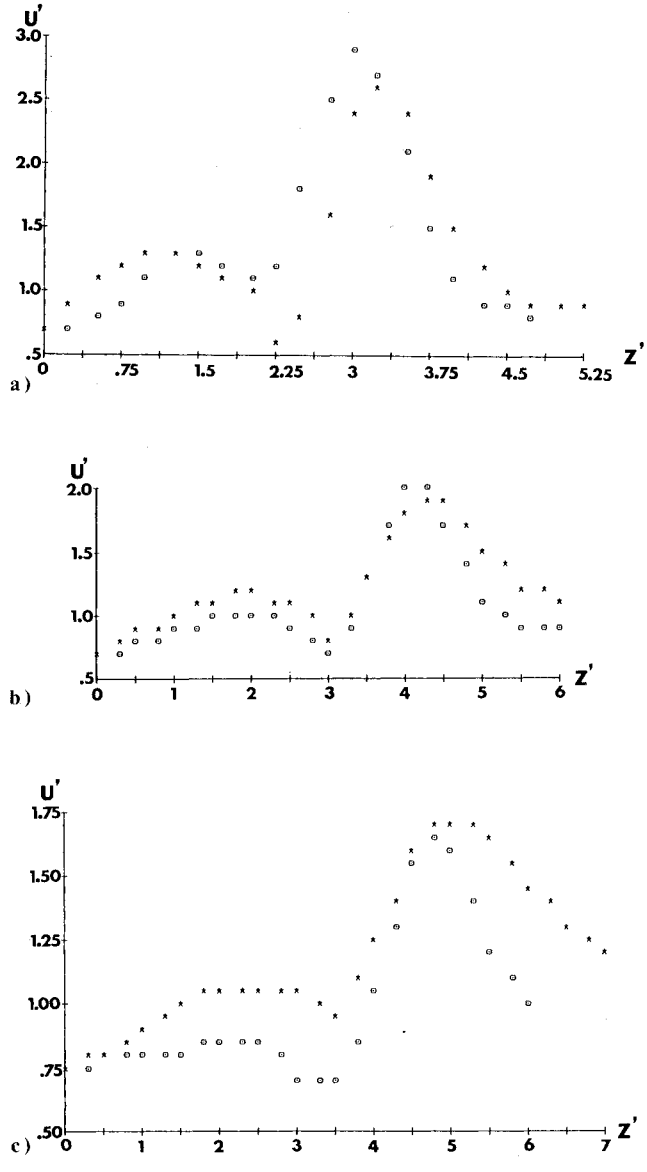

Fig. 6 Comparison between experimental data (o) and results of the mathematical model (*) for the plane $Y' = 0$: a) $X' = 1$; b) $X' = 2$; c) $X' = 3$.

B. Flow Regions

The distributions of the turbulence intensity $T/U = (\bar{u'}^2)^{1/2}/U$, where $\bar{u}'$ is the fluctuating part of the instantaneous velocity, and U' vs Z', are shown together in Fig. 5b for $X' = 2$ and $Y' = 0$ in order to show how the flow regions were defined. There are three maxima in the turbulence distributions. The maximum of T/U is looked upon as a region of high-turbulent shear existing on the boundary between flows displaying very different dynamical characteristics. Hence, the maximum values of T/U are taken as the boundaries of the four flow regions described earlier.

The freestream region is from $Z' = \infty$ to $Z' = 5$, where the first maximum T/U value occurs. The region between the first and second maximum T/U, $3 \leq Z' \leq 5$ is defined as the jet region, and between the second and third maximum T/U value, $3 \geq Z' \geq 1$ as the vortex region. After the vortex region, for $Z' \leq 1$, the wake region is defined.

C. Measured Velocity Distributions

Experimental mean velocity distributions U' vs Z' for $Y'=0$ and for planes $X'=1$, 2, and 3 are shown in Fig. 6. Two maximum values for every distribution are noticeable. The region around the maximum value on the right-hand side corresponds to the jet region with large momenta. The left-hand hump is a contribution due to the two bound vortices in that region. To the authors' best knowledge, this is the first time the vortex influence has been taken into account in this kind of mathematical modeling, and the first time measurements delineate the presence of the bound vortices.

D. Comparison of Theoretical and Measured Velocity Distributions

Using the mathematical model and experimental measurements of the velocity distribution on the intersection line of the plane $Y'=0$ and the planes $X'=1$, 2, and 3, a value of $\nu_\tau = 0.0455\ m^2/s$ was found to be in best agreement at all three planes. These results and experimental data are shown together in Fig. 6. For $X'=1$ and 2, relatively good agreement is obtained, but the agreement at the plane $X'=3$ is poorer. This is partly due to maintaining ν_τ constant at all planes, knowing well that ν_τ is dependent on the turbulence characteristics.

References

[1] Morton, B.R., "On a Momentum-Mass Flux Diagram for Turbulent Jets, Plumes and Wakes," *Journal of Fluid Mechanics,* Vol. 10, 1961, pp. 101-112.

[2] Hoult, D.P., Fay, J.A., and Forney, L.J., "A Theory of Plume Rise Compared with Field Observations," *Journal of Air Pollution Control Association,* Vol. 19, No. 8, 1969, pp. 585-590.

[3] Pratte, B.D. and Baines, W.D., "Profiles of the Round Turbulent Jet in a Cross Flow," *Proceedings of the ASCE Journal of the Hydraulics Division,* 1967, pp. 53-64.

[4] Durando, N.A., "Vortices Induced in a Jet by a Subsonic Cross Flow," *AIAA Journal,* Vol. 9, Feb. 1971, pp. 325-327.

[5] Moussa, Z., Trischka, J., and Eskinazi, S., "The Near Field in the Mixing of a Round Jet with a Cross-Stream," *Journal of Fluid Mechanics,* Vol. 80, 1977, pp. 49-80.

[6] Bojic, M., "Two-Dimensional Mathematical Model of a Non-Buoyant Jet in a Cross-Flow," M.S. Thesis, Dept. of Mechanical and Aerospace Engineering, Syracuse Univ., Syracuse, N.Y., 1977.

[7] Chassaing, P., George, J., Claria, A., and Sananes, F., "Physical Characteristics of Subsonic Jet in a Cross-Stream," *Journal of Fluid Mechanics,* Vol. 62, Pt. 1, 1974, pp. 41-64.

[8] Reichardt, H., "Uber eine neue Theorie der freien Turbulenz," *ZAMM* 21, 257, 1941.

[9] Eskinazi, S., *Vector Mechanics of Fluids and Magnetofluids,* Academic Press, Inc., New York, 1967.

[10] White, F., *Viscous Fluid Flow,* McGraw-Hill Book Co., Inc., New York, 1974.